

# **Ditopic *N*-Heterocyclic Pincer Carbene Complexes Containing a Perylene Backbone**

Susanne Langbein, Hubert Wadepohl, Lutz H. Gade\*

Anorganisch-Chemisches Institut, Universität Heidelberg, Im Neuenheimer Feld 270, 69120 Heidelberg, Germany.

## Table of Contents:

Crystallographic data	S2
NMR spectra of new compounds	S7
IR spectra of compounds 3a and 3b	S18
Absorptionspectra of new compounds	S19
Emission and excitation fluorescence spectra of new compounds	S19

Summary of Data CCDC 1442271

---

Compound Name: 1a

Formula: C<sub>74</sub> H<sub>60</sub> N<sub>4</sub> P<sub>4</sub>

Unit Cell Parameters: a 8.02610(19) b 30.4330(7) c 11.5232(2) P21/c

---

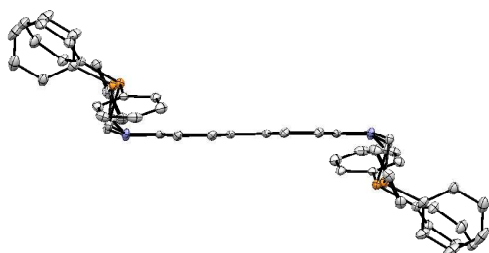


**Figure S 1.** Side view of the molecular structure of **1a**. The ellipsoids are drawn with a 50 % probability level. The hydrogen atoms are omitted for clarity.

Summary of Data CCDC 1442272

---

Compound Name: 1b

Formula: C<sub>74</sub> H<sub>108</sub> N<sub>4</sub> P<sub>4</sub>

Unit Cell Parameters: a 31.8240(9) b 11.1607(4) c 18.8439(4) P21/c

---

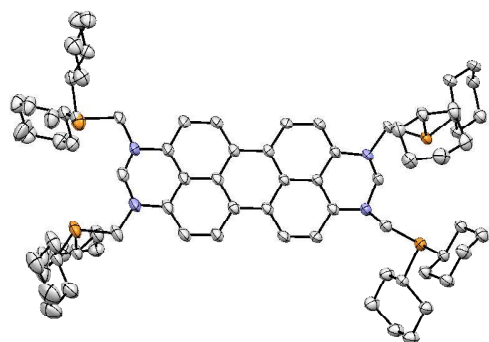


**Figure S 2.** Front view of the molecular structure of **1b**. The ellipsoids are drawn with a 50 % probability level. The hydrogen atoms are omitted for clarity.

#### Summary of Data CCDC 1442273

Compound Name: 1c

Formula: C<sub>50</sub> H<sub>76</sub> N<sub>4</sub> P<sub>4</sub> C<sub>6</sub> H<sub>6</sub>

Unit Cell Parameters: a 35.8845(9) b 15.2434(3) c 9.6886(2) C2/c

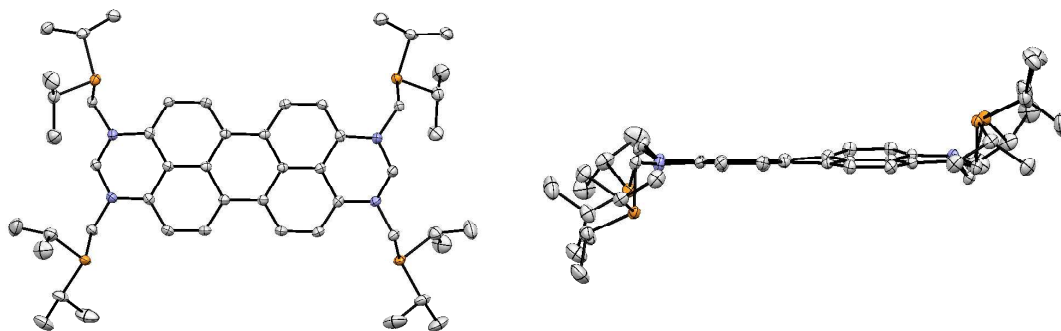


**Figure S 3.** Front view (left) and side view (right) of the molecular structure of **1c**. The ellipsoids are drawn with a 50 % probability level. The hydrogen atoms are omitted for clarity.

#### Summary of Data CCDC 1442274

Compound Name: 2c

Formula: C<sub>50</sub> H<sub>72</sub> Cl<sub>2</sub> N<sub>4</sub> P<sub>4</sub> Rh<sub>2</sub> C<sub>4</sub> H<sub>8</sub> O<sub>1</sub>

Unit Cell Parameters: a 27.9454(3) b 13.70389(12) c 15.62974(19) Pna21

#### X-ray Crystal Structure Determinations

Crystal data and details of the structure determinations are compiled in Table S1. Full shells of intensity data were collected at low temperature with an Agilent Technologies Supernova-E CCD diffractometer (Mo- or Cu- $K_{\alpha}$  radiation, microfocus X-ray tube, multilayer mirror optics). Data were corrected for air and detector absorption, Lorentz and polarization effects;<sup>1</sup> absorption by the crystal was treated numerically (Gaussian grid).<sup>1,2</sup> The structures were solved by “modern” direct methods (compound 1b)<sup>3</sup> or by the charge flip procedure (all other compounds)<sup>4</sup> and refined by full-matrix least squares methods based on  $F^2$  against all unique reflections.<sup>5</sup> All non-hydrogen atoms were given anisotropic displacement parameters. Hydrogen atoms were generally input at calculated positions and refined with a riding model. For compound 1a the positions of the hydrogen atoms were taken from difference Fourier syntheses and refined. When found necessary, disordered groups and/or solvent molecules were subjected to suitable geometry and adp restraints.

Due to severe disorder and fractional occupancy, electron density attributed to solvent of crystallization (thf) was removed from the structure of 2c with the BYPASS procedure,<sup>6</sup> as implemented in PLATON (SQUEEZE).<sup>7</sup> Partial structure factors from the solvent masks were included in the refinement as separate contributions to  $F_{\text{obs}}$ .

- 1 *CrysAlisPro*, Agilent Technologies UK Ltd., Oxford, UK 2011-2014 and Rigaku Oxford Diffraction, Rigaku Polska Sp.z o.o., Wrocław, Poland 2015.
- 2 Busing, W. R.; Levy, H. A. *Acta Cryst.* 1957, *10*, 180.
- 3 (a) Burla, M. C.; Caliandro, R.; Carrozzini, B.; Cascarano, G. L.; Cuocci, C.; Giacovazzo, C.; Mallamo, M.; Mazzone, A.; Polidori, G. *SIR2014*, CNR IC, Bari, Italy, 2014; (b) Burla, M. C.; Caliandro, R.; Carrozzini, B.; Cascarano, G. L.; Cuocci, C.; Giacovazzo, C.; Mallamo, M.; Mazzone, A.; Polidori, G. *J. Appl. Cryst.* 2015, *48*, 306.
- 4 (a) Palatinus, L. *SUPERFLIP*, EPF Lausanne, Switzerland and Fyzikální ústav AV ČR, v. v. i., Prague, Czech Republic, 2007-2014 (b) Palatinus, L.; Chapuis, G. *J. Appl. Cryst.* 2007, *40*, 786.
- 5 (a) Sheldrick, G. M. *SHELXL-20xx*, University of Göttingen and Bruker AXS GmbH, Karlsruhe, Germany 2012-2014; (b) Sheldrick, G. M. *Acta Cryst.* 2008, *A64*, 112; (c) Sheldrick, G. M. *Acta Cryst.* 2015, *C71*, 3.
- 6 (a) v. d. Sluis, P.; Spek, A. L. *Acta Cryst.* 1990, *A46*, 194; (b) Spek, A. L. *Acta Cryst.* 2015, *C71*, 9.
- 7 (a) Spek, A. L. *PLATON*, Utrecht University, The Netherlands; (b) Spek, A. L. *J. Appl. Cryst.* 2003, *36*, 7.

**Table S 1. Details of the crystal structure determinations of 1a, 1b.**

	<b>1a</b>	<b>1b</b>
formula	C <sub>74</sub> H <sub>60</sub> N <sub>4</sub> P <sub>4</sub>	C <sub>74</sub> H <sub>108</sub> N <sub>4</sub> P <sub>4</sub>
crystal system	monoclinic	monoclinic
space group	<i>P</i> 2 <sub>1</sub> / <i>c</i>	<i>P</i> 2 <sub>1</sub> / <i>c</i>
<i>a</i> [Å]	8.02610(19)	31.8240(9)
<i>b</i> [Å]	30.4330(7)	11.1607(4)
<i>c</i> [Å]	11.5232(2)	18.8439(4)
$\beta$ [°]	91.934(2)	95.693(2)
<i>V</i> [Å <sup>3</sup> ]	2813.04(11)	6660.0(3)
<i>Z</i>	2	4
<i>M<sub>r</sub></i>	1129.14	1177.52
<i>F</i> <sub>000</sub>	1184	2560
<i>d<sub>c</sub></i> [Mg·m <sup>-3</sup> ]	1.333	1.174
$\mu$ [mm <sup>-1</sup> ]	0.185	1.378
max., min. transmission factors	0.997, 0.981	0.971, 0.865
X-radiation, $\lambda$ [Å]	Mo- <i>K</i> $\alpha$ , 0.71073	Cu- <i>K</i> $\alpha$ , 1.54184
data collect. temperat. [K]	110(1)	120(1)
$\theta$ range [°]	3.2 to 28.3	4.2 to 67.1
index ranges <i>h,k,l</i>	-10 ... 10, -39 ... 38, -14 ... 15	-38 ... 38, -13 ... 13, -22 ... 22
reflections measured	54562	353291
unique [ <i>R</i> <sub>int</sub> ]	6829 [0.0858]	11897 [0.1705]
observed [ <i>I</i> ≥ 2 $\sigma$ ( <i>I</i> )]	5120	8462
data / restraints / parameters	6829 / 0 / 460	11897 / 955 / 884
GooF on <i>F</i> <sup>2</sup>	1.027	1.042
<i>R</i> indices [ <i>F</i> > 4 $\sigma$ ( <i>F</i> )] <i>R</i> ( <i>F</i> ), <i>wR</i> ( <i>F</i> <sup>2</sup> )	0.0489, 0.0974	0.0685, 0.1612
<i>R</i> indices (all data) <i>R</i> ( <i>F</i> ), <i>wR</i> ( <i>F</i> <sup>2</sup> )	0.0743, 0.1078	0.1018, 0.1792
absolute structure parameter		
largest residual peaks [e·Å <sup>-3</sup> ]	0.407, -0.314	1.148, -0.394

**Table S 2. Details of the crystal structure determinations of 1c, 2c.**

	<b>1c</b>	<b>2c</b>
formula	C <sub>56</sub> H <sub>82</sub> N <sub>4</sub> P <sub>4</sub>	C <sub>58</sub> H <sub>88</sub> Cl <sub>2</sub> N <sub>4</sub> O <sub>2</sub> P <sub>4</sub> Rh <sub>2</sub>
crystal system	monoclinic	orthorhombic
space group	<i>C</i> 2/ <i>c</i>	<i>P</i> <i>na</i> 2 <sub>1</sub>
<i>a</i> [Å]	35.8845(9)	27.9454(3)
<i>b</i> [Å]	15.2434(3)	13.70389(12)
<i>c</i> [Å]	9.6886(2)	15.62974(19)
$\beta$ [°]	91.239(2)	
<i>V</i> [Å <sup>3</sup> ]	5298.5(2)	5985.58(11)
<i>Z</i>	4	4
<i>M<sub>r</sub></i>	935.13	1273.92
<i>F</i> <sub>000</sub>	2024	2656
<i>d<sub>c</sub></i> [Mg·m <sup>-3</sup> ]	1.172	1.414
$\mu$ [mm <sup>-1</sup> ]	1.608	0.791
max., min. transmission factors	0.965, 0.808	0.967, 0.912
X-radiation, $\lambda$ [Å]	Cu- <i>K</i> $\alpha$ , 1.54184	Mo- <i>K</i> $\alpha$ , 0.71073
data collect. temperat. [K]	120(1)	120(1)
$\theta$ range [°]	4.7 to 70.7	3.3 to 30.5
index ranges <i>h,k,l</i>	-41 ... 43, -18 ... 18, -11 ... 11	-39 ... 39, -19 ... 19, -22 ... 22
reflections measured	69633	324309
unique [ <i>R</i> <sub>int</sub> ]	5072 [0.0549]	18298 [0.0780]
observed [ <i>I</i> ≥ 2 $\sigma$ ( <i>I</i> )]	4271	16545
data / restraints / parameters	5072 / 36 / 312	18298 / 634 / 631
GooF on <i>F</i> <sup>2</sup>	1.025	1.023
<i>R</i> indices [ <i>F</i> > 4 $\sigma$ ( <i>F</i> )] <i>R</i> ( <i>F</i> ), <i>wR</i> ( <i>F</i> <sup>2</sup> )	0.0338, 0.0848	0.0486, 0.1245
<i>R</i> indices (all data) <i>R</i> ( <i>F</i> ), <i>wR</i> ( <i>F</i> <sup>2</sup> )	0.0431, 0.0898	0.0546, 0.1282
absolute structure parameter		0.050(8)
largest residual peaks [e·Å <sup>-3</sup> ]	0.270, -0.189	2.987, -0.840

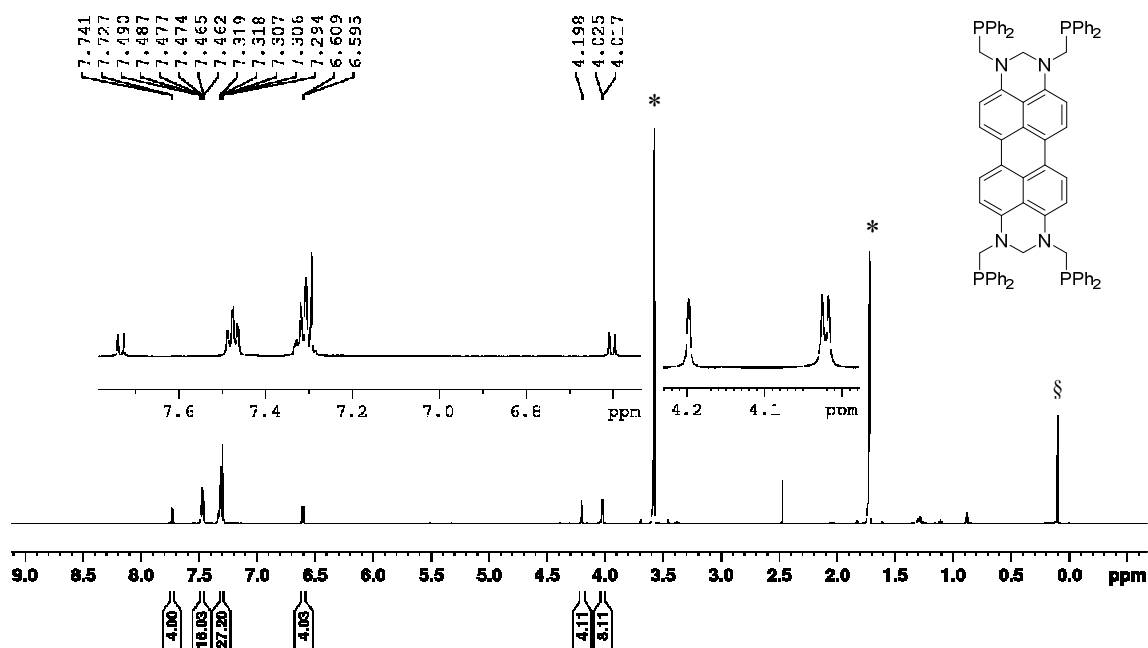


**Figure S 4.** <sup>1</sup>H NMR (600.13 MHz, THF-d<sub>8</sub>) of **1a**. Silicon grease is labelled with § and residual proton signals of THF-d<sub>8</sub> are labelled with \*.

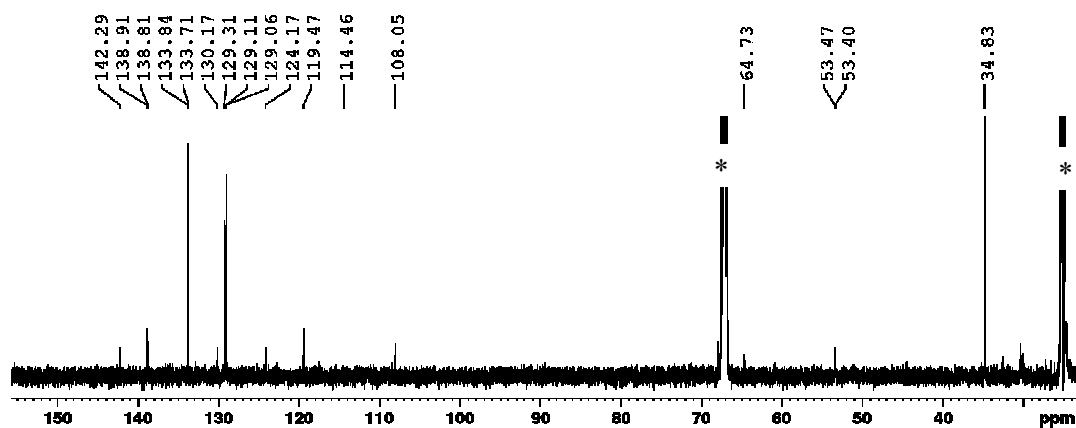


**Figure S 5.** <sup>13</sup>C NMR (150.90 MHz, THF-d<sub>8</sub>) of **1a**. Residual carbon signals of THF-d<sub>8</sub> are labelled with \*.

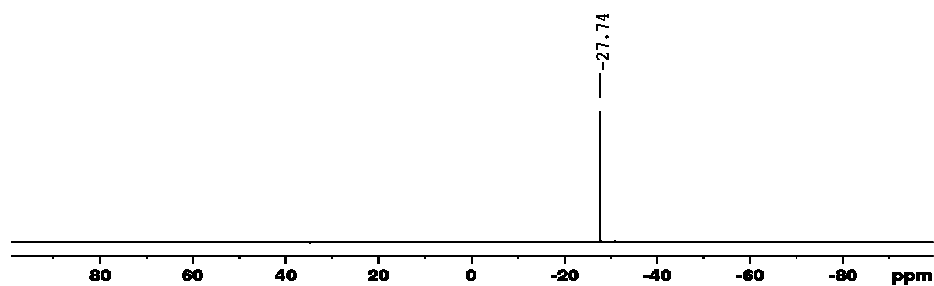


**Figure S 6.** <sup>31</sup>P NMR (242.94 MHz, THF-d<sub>8</sub>) of **1a**.

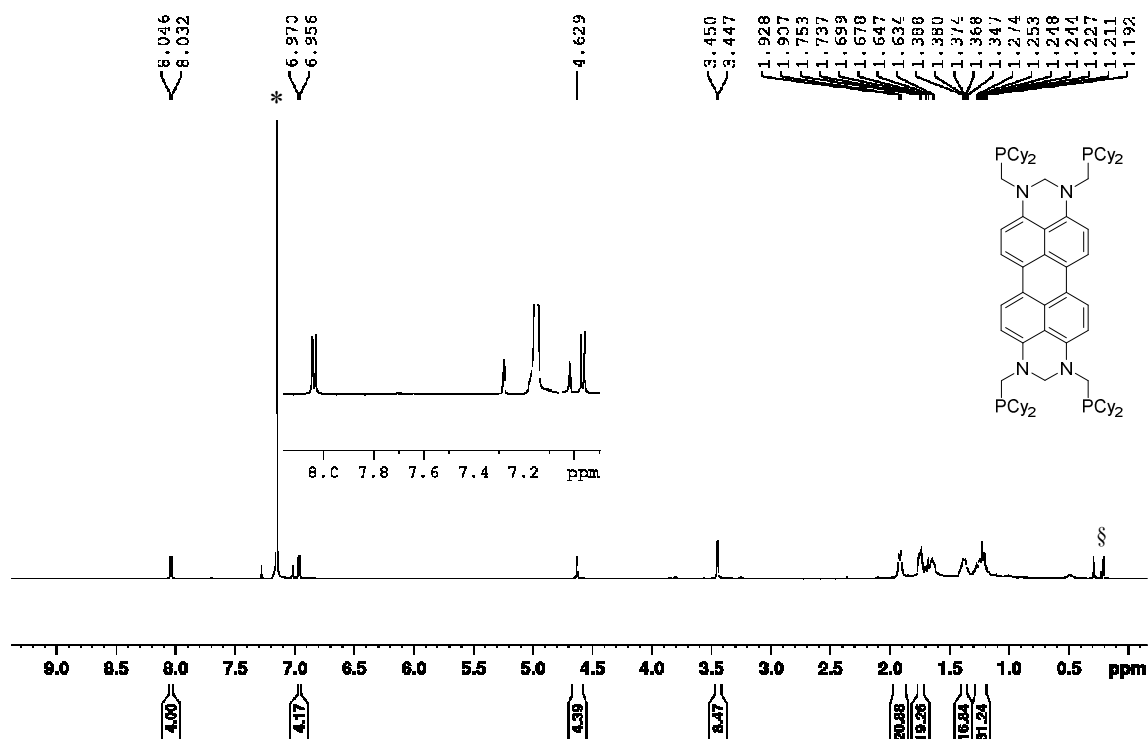


**Figure S 7.** <sup>1</sup>H NMR (600.13 MHz, C<sub>6</sub>D<sub>6</sub>) of **1b**. Silicon grease is labelled with § and residual proton signal of C<sub>6</sub>D<sub>6</sub> with \*.

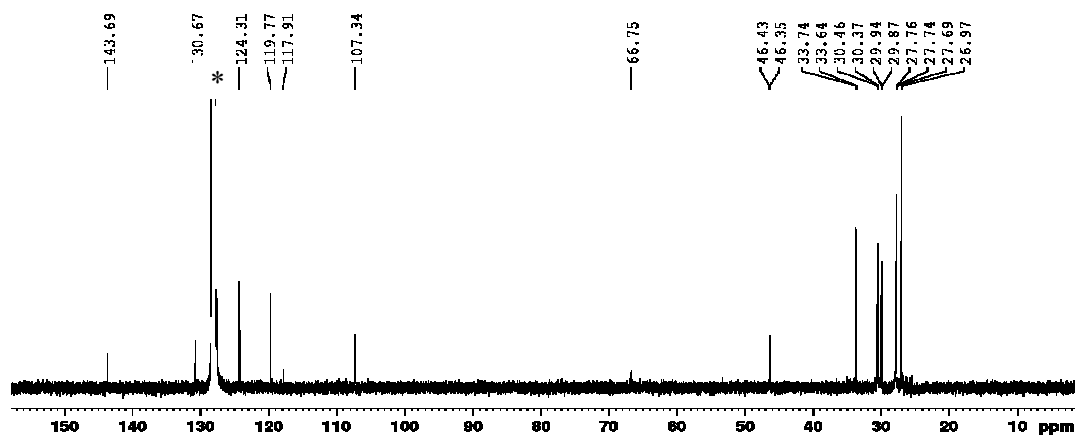


**Figure S 8.** <sup>13</sup>C NMR (150.90 MHz, C<sub>6</sub>D<sub>6</sub>) of **1b**. Residual carbon signal of C<sub>6</sub>D<sub>6</sub> is labelled with \*.

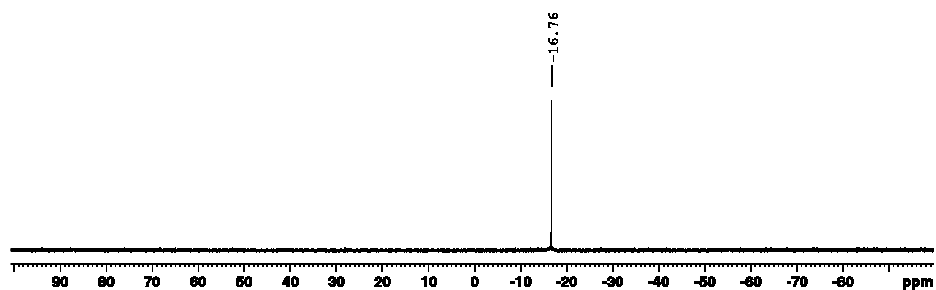


**Figure S 9.** <sup>31</sup>P NMR (242.94 MHz, C<sub>6</sub>D<sub>6</sub>) of **1b**.



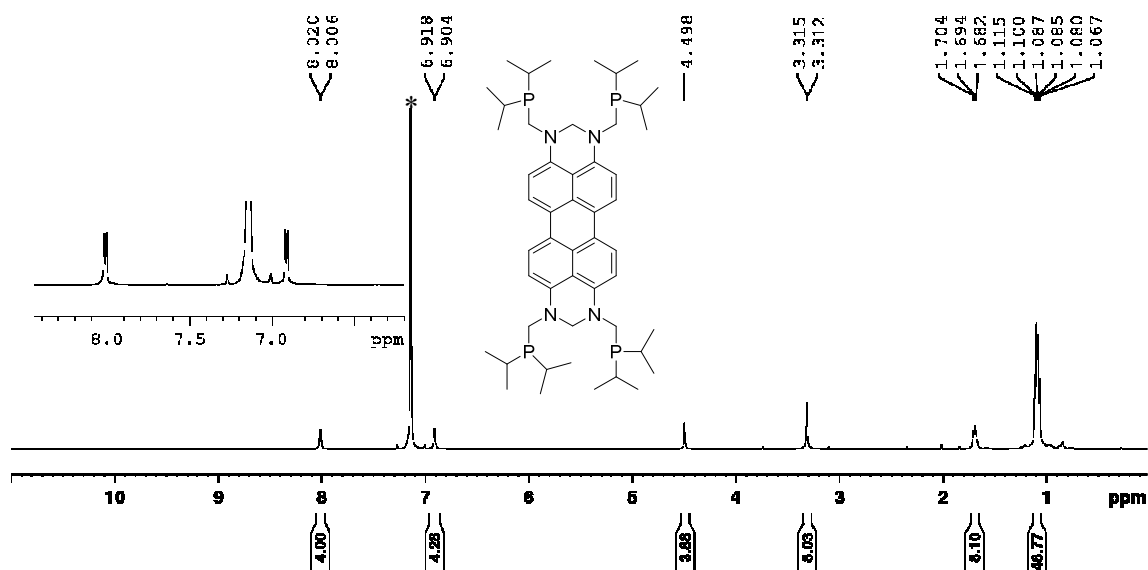


Figure S 10. <sup>1</sup>H NMR (600.13 MHz, C<sub>6</sub>D<sub>6</sub>) of **1c**. Residual proton signal of C<sub>6</sub>D<sub>6</sub> is labelled with \*.

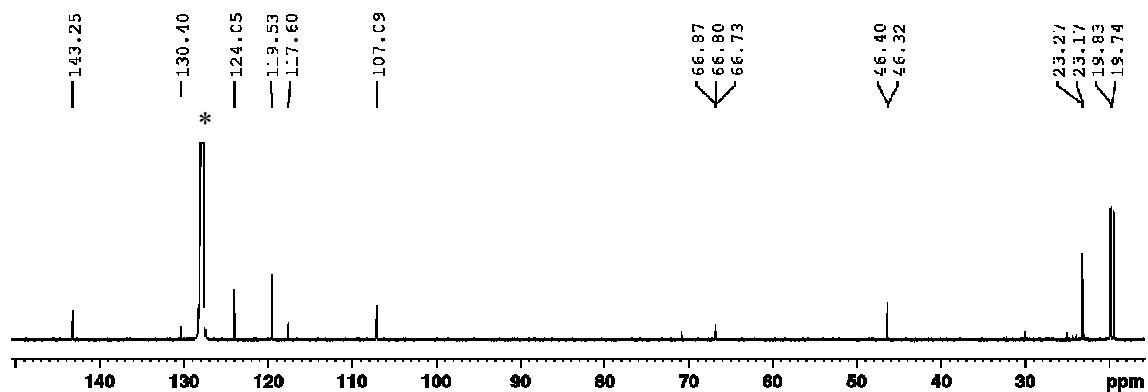


Figure S 11. <sup>13</sup>C NMR (150.90 MHz, C<sub>6</sub>D<sub>6</sub>) of **1c**. Residual carbon signal of C<sub>6</sub>D<sub>6</sub> is labelled with \*.

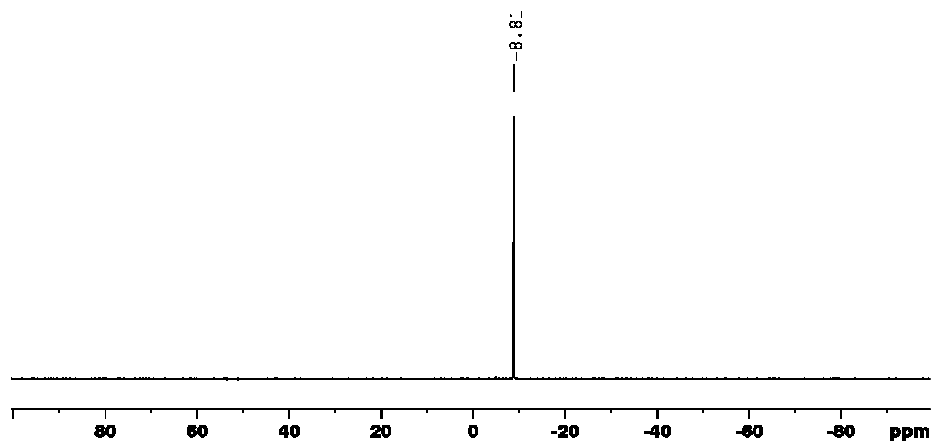
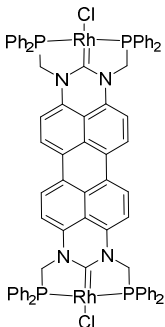


Figure S 12. <sup>31</sup>P NMR (242.94 MHz, C<sub>6</sub>D<sub>6</sub>) of **1c**.



**Figure S 14.**  $^{13}\text{C}$  NMR (150.90 MHz,  $\text{CD}_2\text{Cl}_2$ ) of **2a**. Residual carbon signal of  $\text{C}_2\text{Cl}_2$  is labelled with \*.

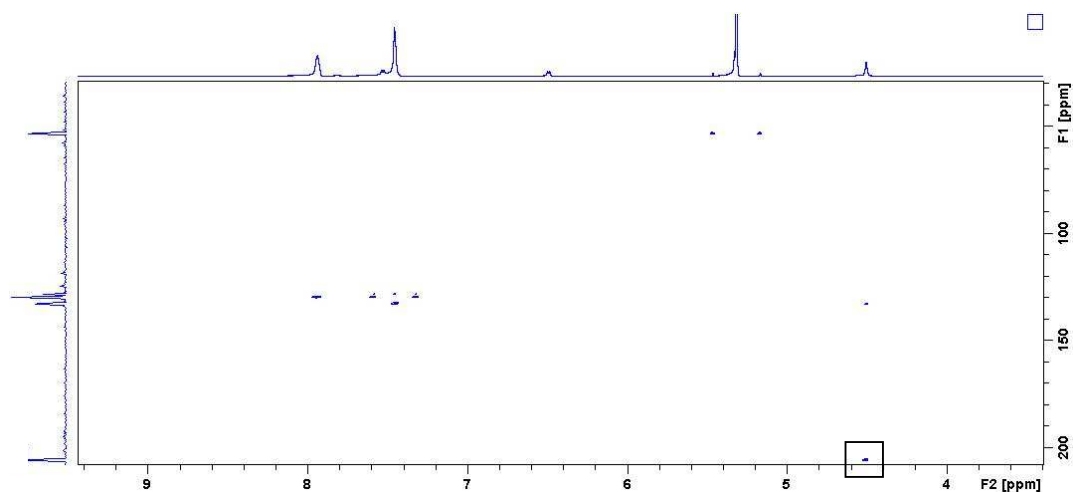


Figure S 15. 2D HMBC NMR (600.13 MHz/150.90 MHz,  $\text{CD}_2\text{Cl}_2$ ) of **2a**.

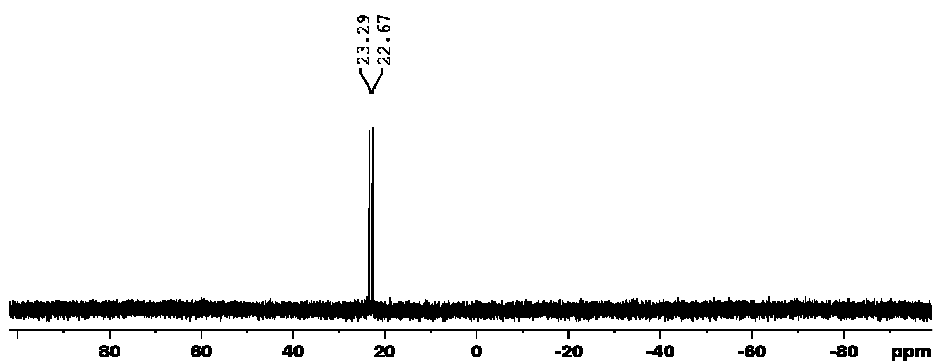


Figure S 16.  $^{31}\text{P}$  NMR (242.94 MHz,  $\text{CD}_2\text{Cl}_2$ ) of **2a**.

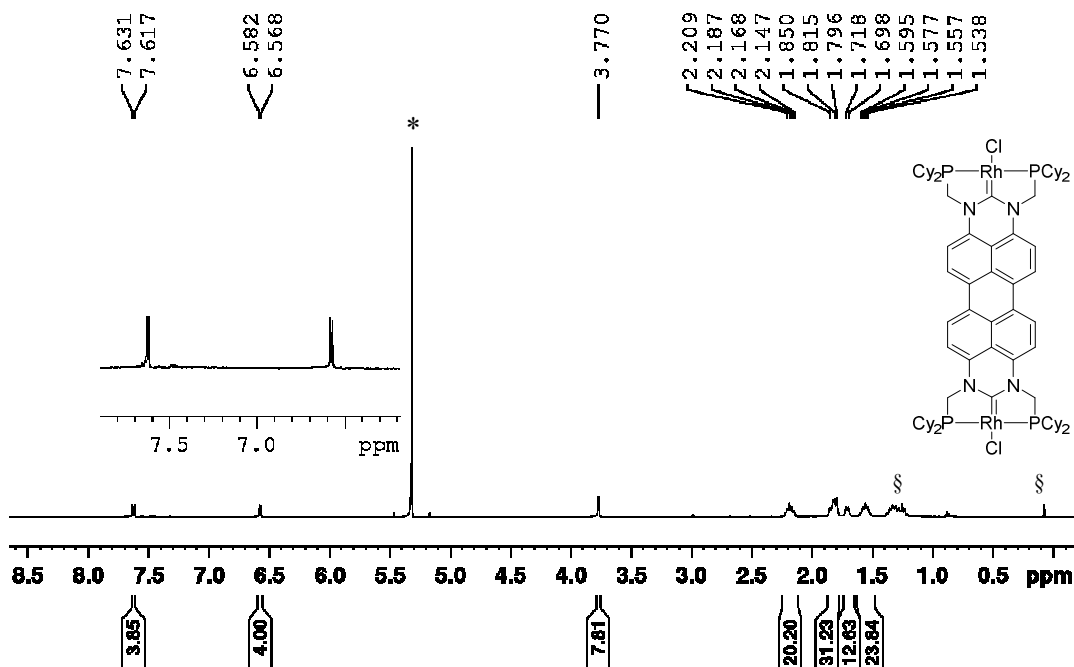


Figure S 17.  $^1\text{H}$  NMR (600.13 MHz,  $\text{CD}_2\text{Cl}_2$ ) of **2b**. Silicon grease and residual hexane are labelled with § and residual proton signal of  $\text{C}_2\text{Cl}_2$  with \*.

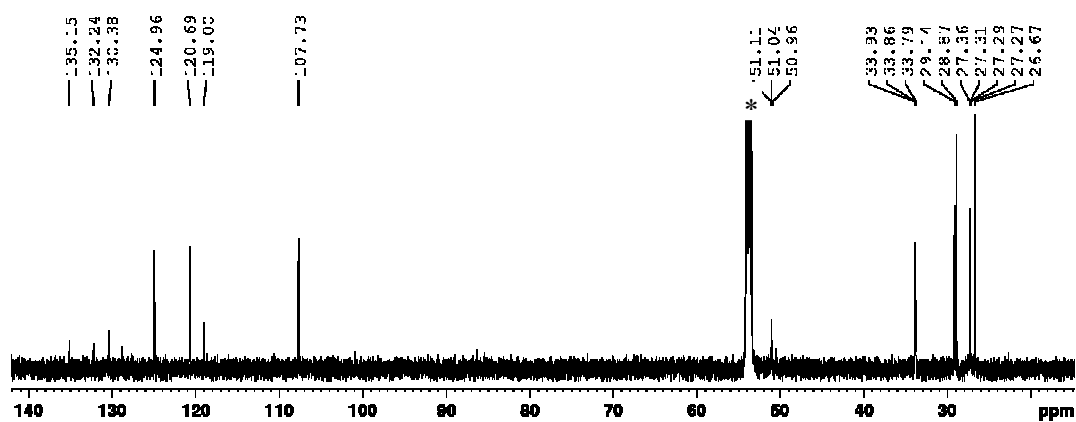


Figure S 18.  $^{13}\text{C}$  NMR (150.90 MHz,  $\text{CD}_2\text{Cl}_2$ ) of **2b**. Residual carbon signal of  $\text{C}_2\text{Cl}_2$  is labelled with \*.

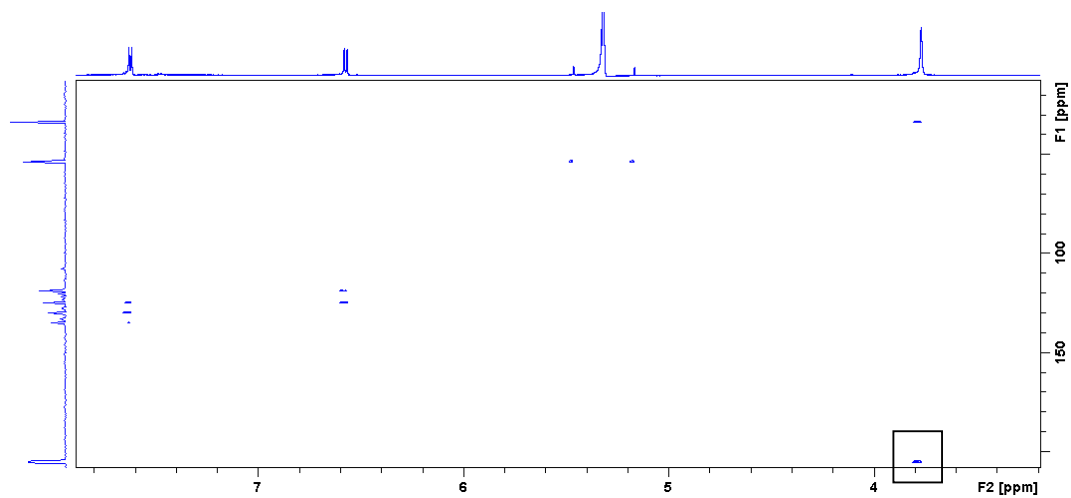


Figure S 19. Detail of 2D HMBC NMR (600.13 MHz/150.90 MHz,  $\text{CD}_2\text{Cl}_2$ ) of **2b**.

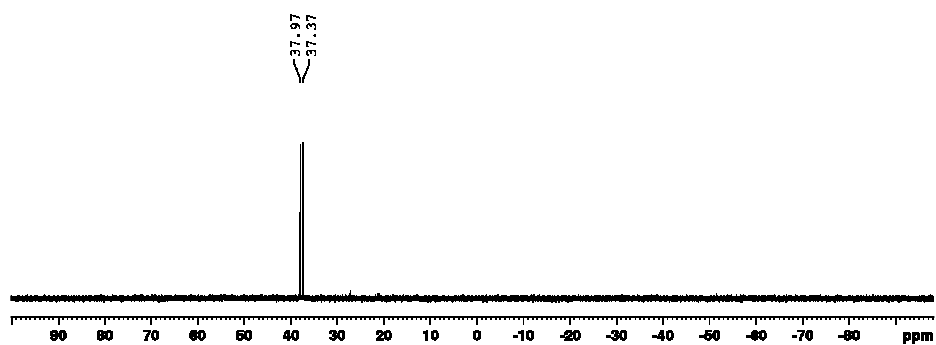
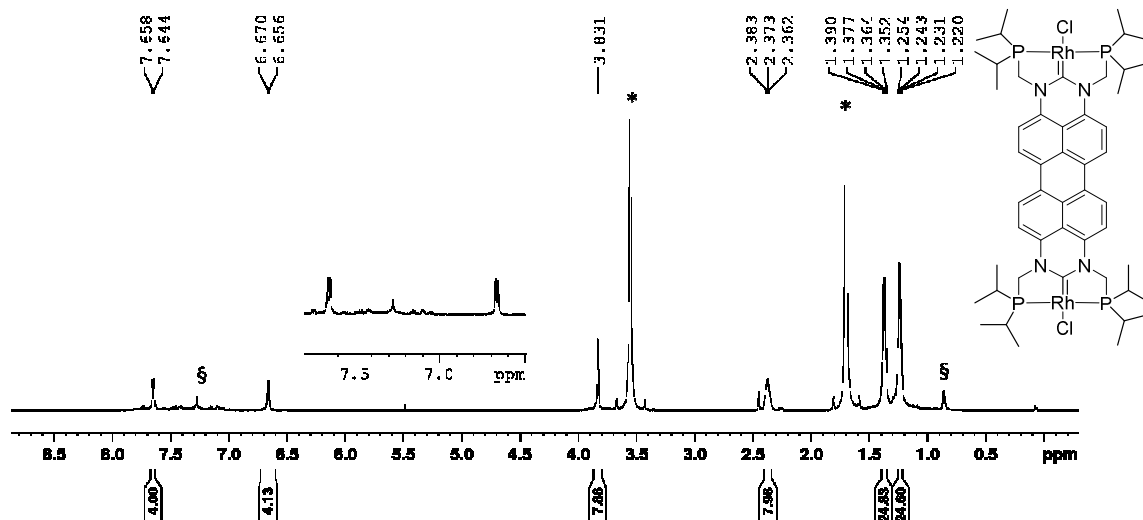
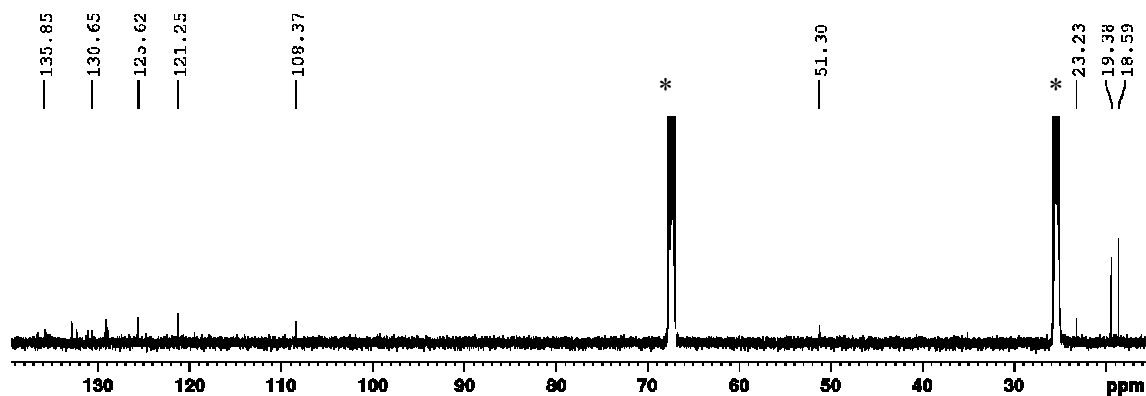


Figure S 20.  $^{31}\text{P}$  NMR (242.94 MHz,  $\text{CD}_2\text{Cl}_2$ ) of **2b**.



**Figure S 21.**  $^1\text{H}$  NMR (600.13 MHz,  $\text{THF-d}_8$ ) of **2c**. Silicon grease and unknowns impurities of the solvent are labelled with § and residual proton signal of  $\text{THF-d}_8$  with \*.



**Figure S 22.**  $^{13}\text{C}$  NMR (150.90 MHz,  $\text{THF-d}_8$ ) of **2c**. Residual carbon signal of  $\text{THF-d}_8$  is labelled with \*.

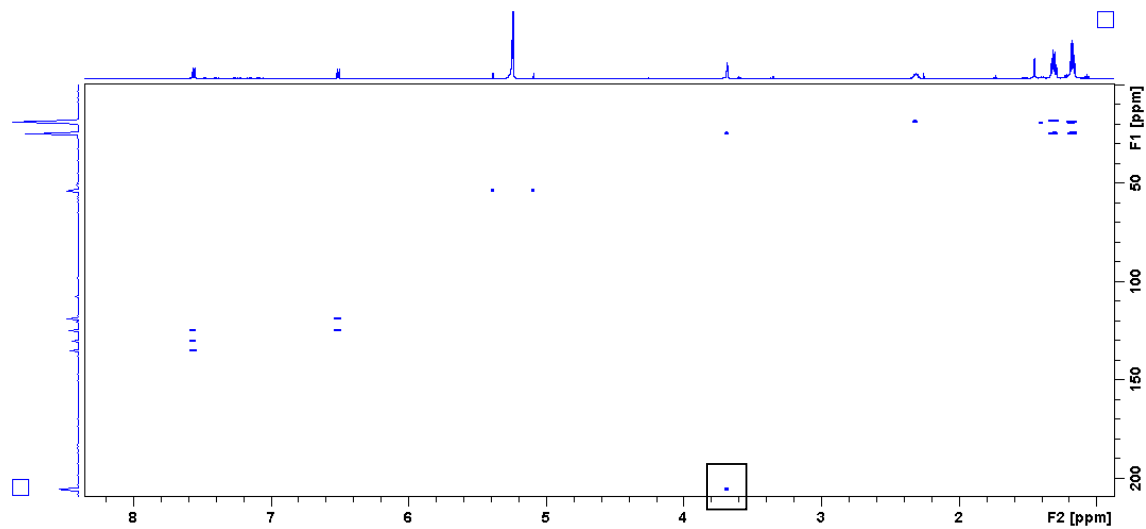


**Figure S 23.** Detail of 2D HMBC NMR (600.13 MHz/150.90 MHz,  $\text{CD}_2\text{Cl}_2$ ) of **2c**.

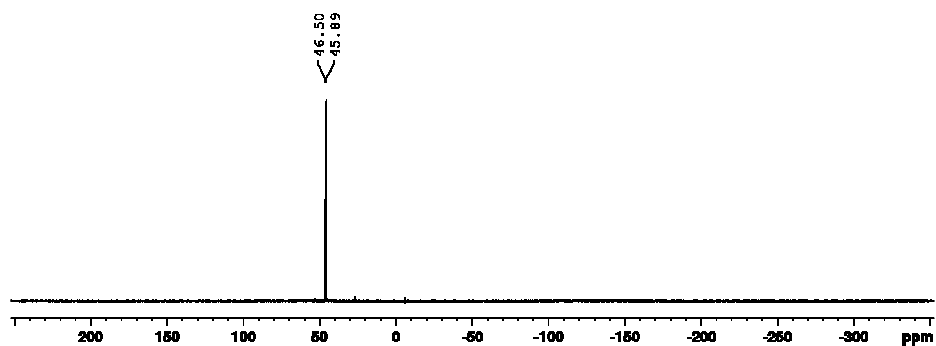


Figure S 24.  $^{31}\text{P}$  NMR (242.94 MHz,  $\text{CD}_2\text{Cl}_2$ ) of **2c**.

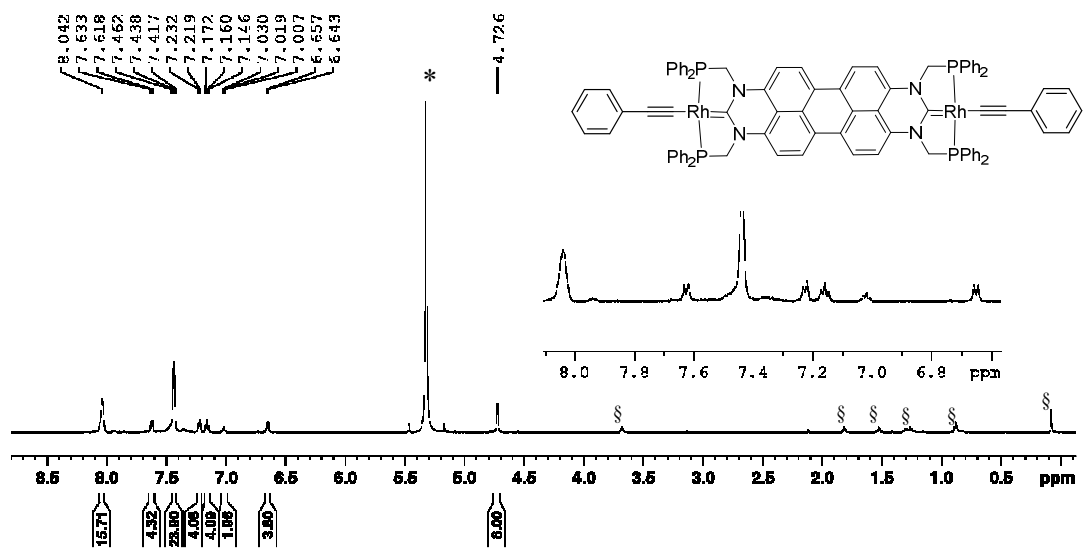


Figure S 25.  $^1\text{H}$  NMR (600.13 MHz,  $\text{CD}_2\text{Cl}_2$ ) of **3a**. Silicon grease and unknowns impurities are labelled with § and residual proton signal of  $\text{CD}_2\text{Cl}_2$  with \*.

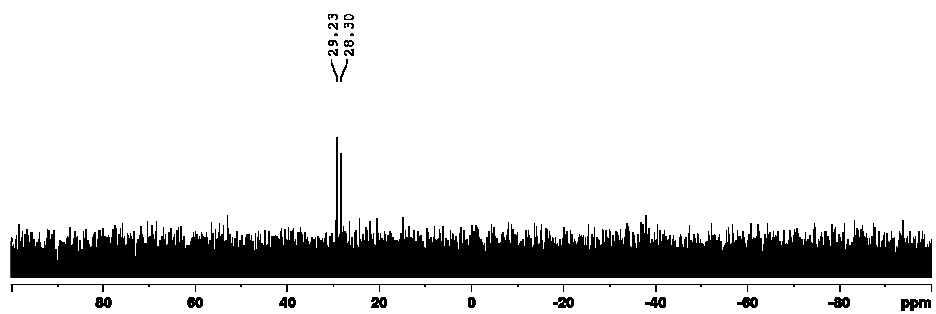
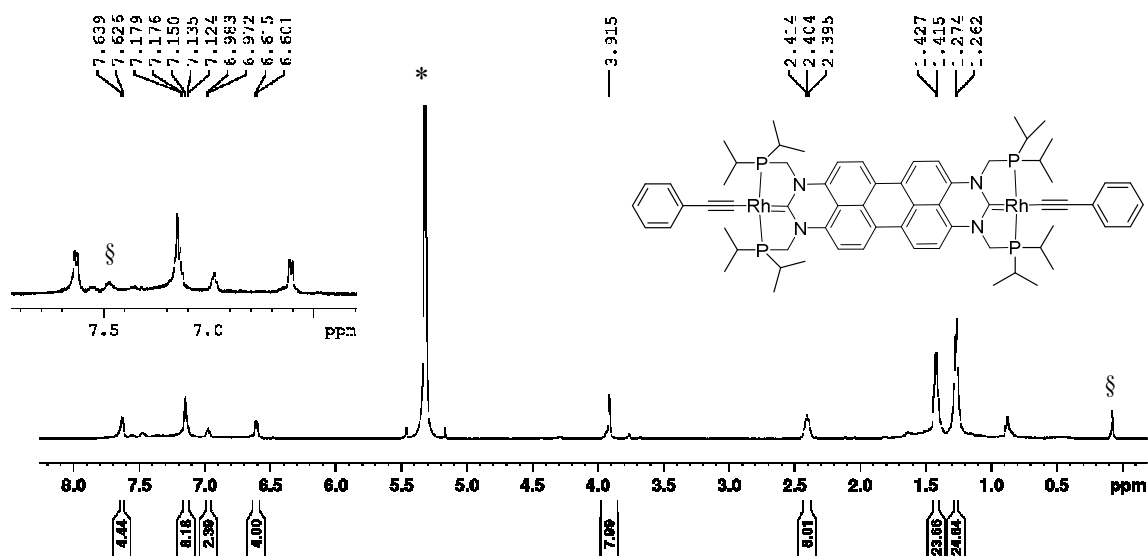
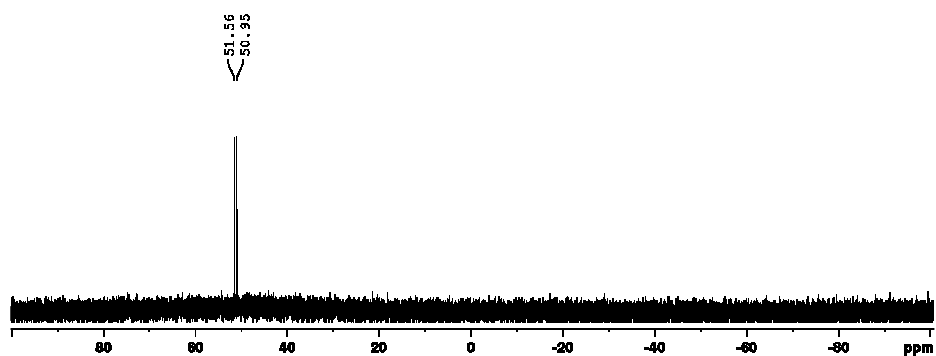


Figure S 26.  $^{31}\text{P}$  NMR (242.94 MHz,  $\text{CD}_2\text{Cl}_2$ ) of **3a**.



**Figure S 27.** <sup>1</sup>H NMR (600.13 MHz, CD<sub>2</sub>Cl<sub>2</sub>) of **3b**. Silicon grease and unknown impurities are labelled with § and residual proton signal of CD<sub>2</sub>Cl<sub>2</sub> with \*.



**Figure S 28.** <sup>31</sup>P NMR (242.94 MHz, CD<sub>2</sub>Cl<sub>2</sub>) of **3b**.

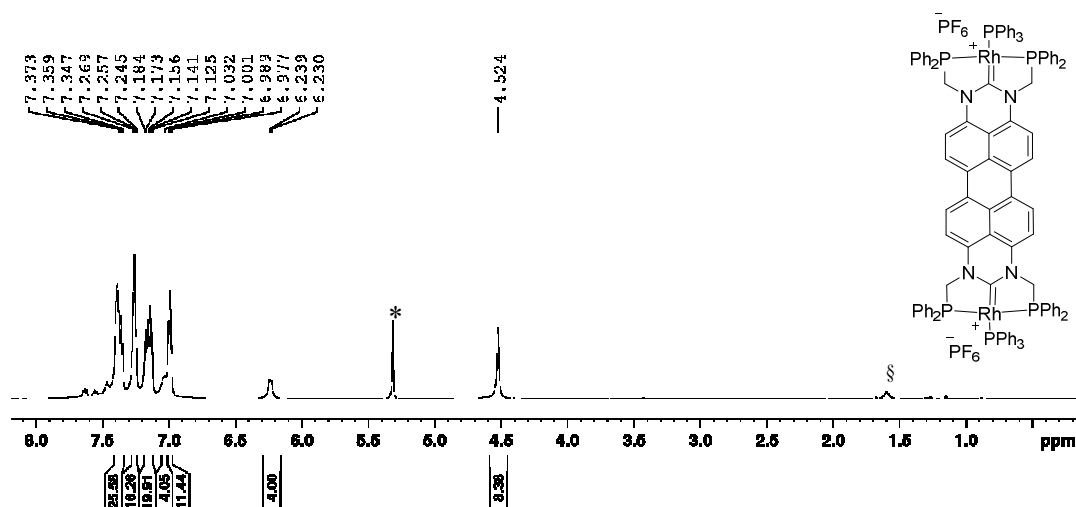


**Figure S 29.** <sup>1</sup>H NMR (600.13 MHz, CD<sub>2</sub>Cl<sub>2</sub>) of **4a**. Unknown impurities are labelled with § and residual proton signal of CD<sub>2</sub>Cl<sub>2</sub> with \*.

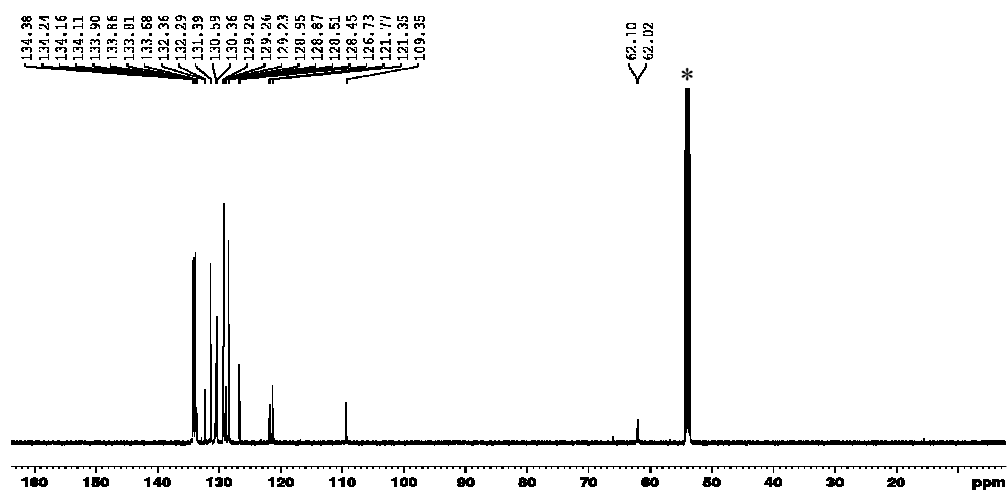


Figure S 30.  $^{13}\text{C}$  NMR (150.90 MHz,  $\text{CD}_2\text{Cl}_2$ ) of **4a**. Residual proton signal of  $\text{THF-d}_8$  with \*.

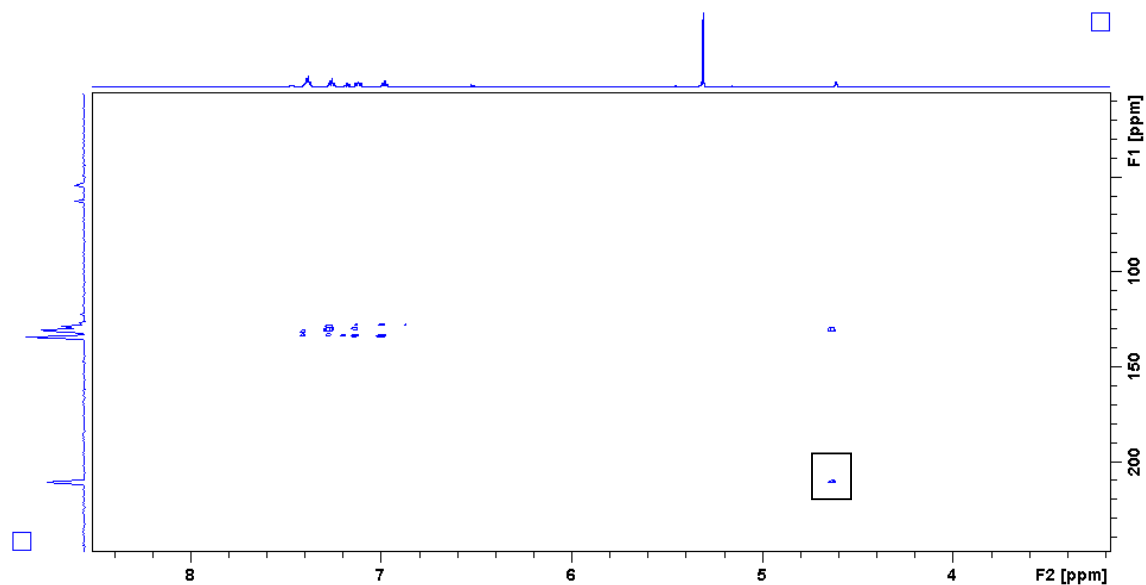


Figure S 31. Detail of 2D HMBC NMR (600.13 MHz/150.90 MHz,  $\text{CD}_2\text{Cl}_2$ ) of **4a**.

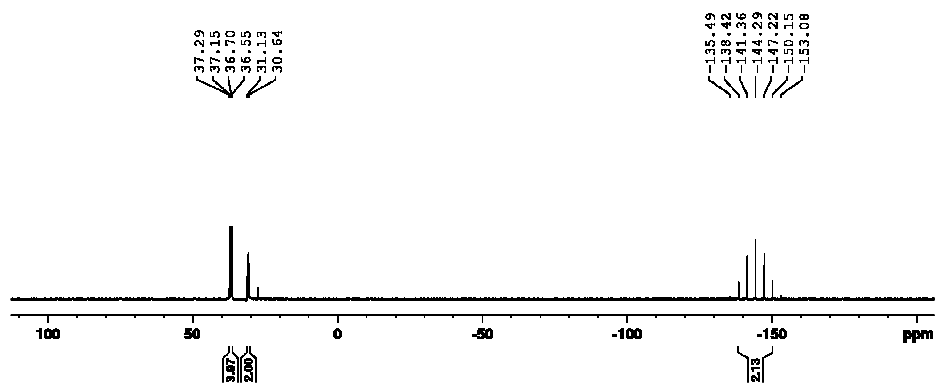
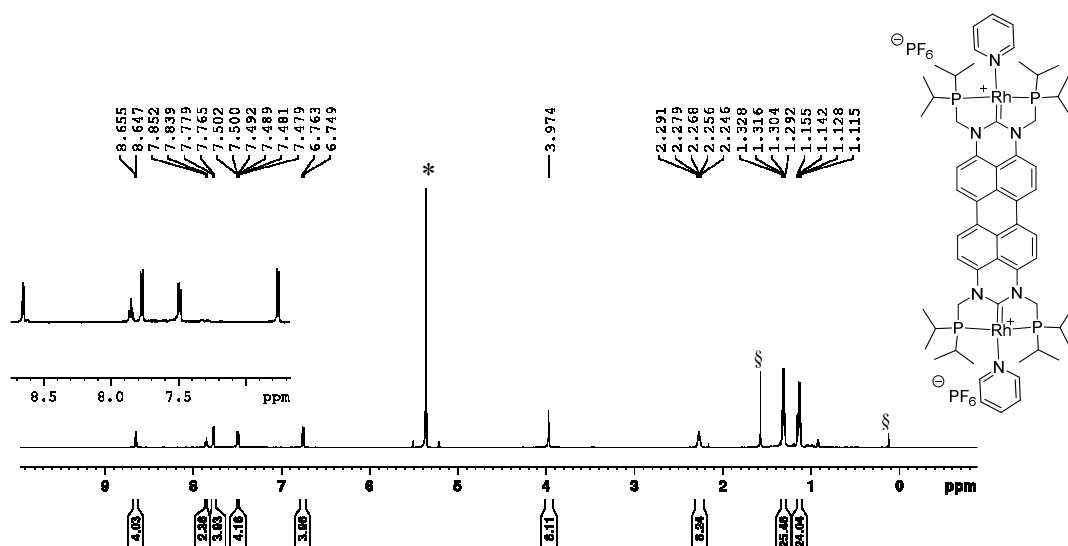
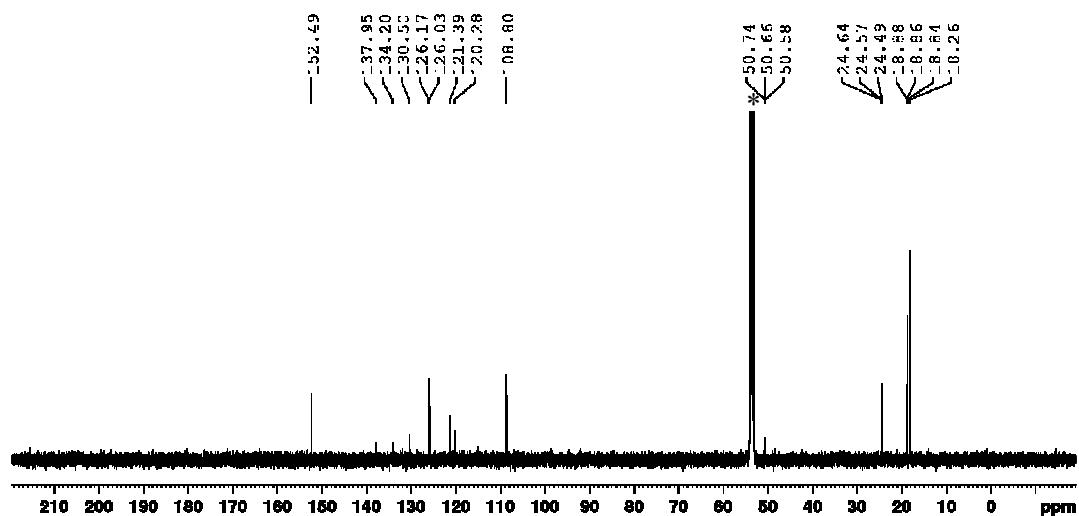


Figure S 32.  $^{31}\text{P}$  NMR (242.94 MHz,  $\text{CD}_2\text{Cl}_2$ ) of **4a**.





**Figure S 33.** <sup>1</sup>H NMR (600.13 MHz, CD<sub>2</sub>Cl<sub>2</sub>) of **4b**. Water and silicon grease are labelled with § and residual proton signal of CD<sub>2</sub>Cl<sub>2</sub> with \*.



**Figure S 34.** <sup>13</sup>C NMR (150.90 MHz, CD<sub>2</sub>Cl<sub>2</sub>) of **4b**. Residual proton signal of THF-d<sub>8</sub> with \*.

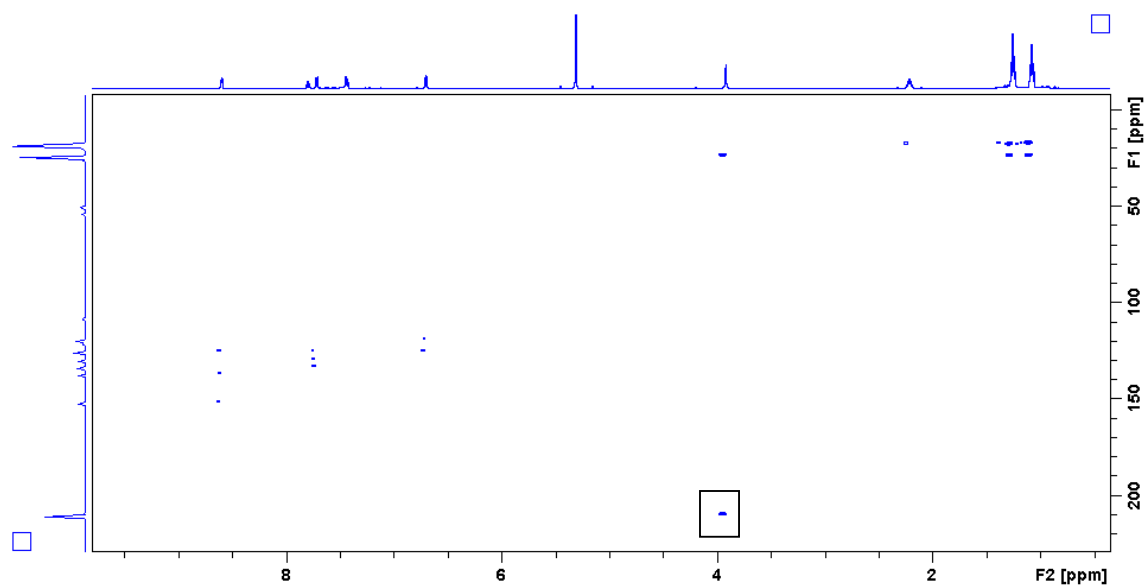


Figure S 35. Detail of 2D HMBC NMR (600.13 MHz/150.90 MHz,  $\text{CD}_2\text{Cl}_2$ ) of **4b**.

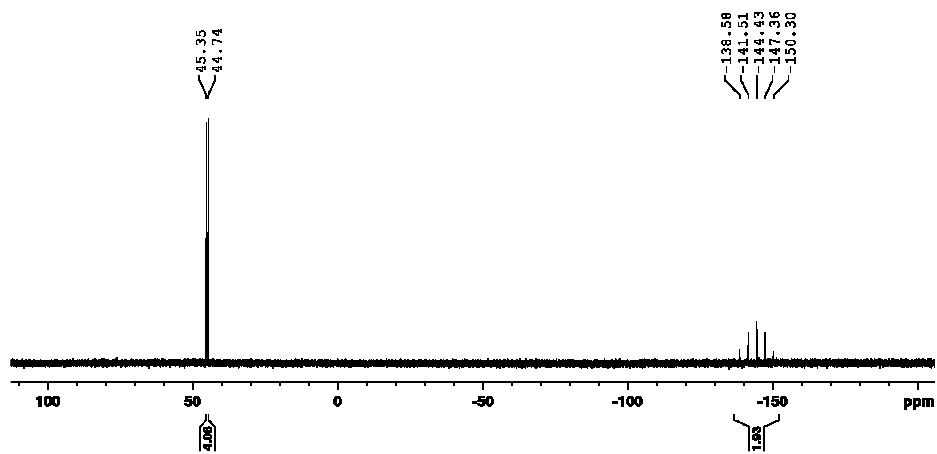


Figure S 36.  $^{31}\text{P}$  NMR (242.94 MHz,  $\text{CD}_2\text{Cl}_2$ ) of **4b**.

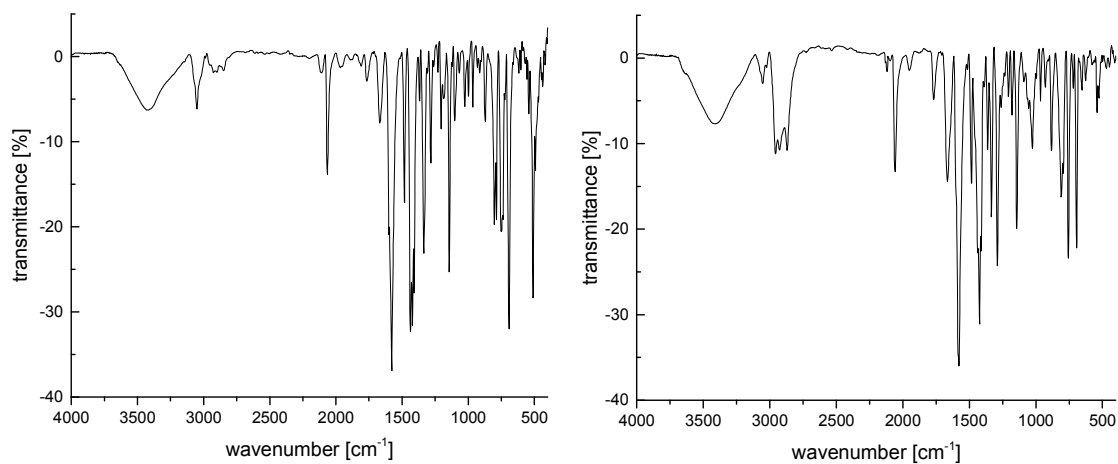
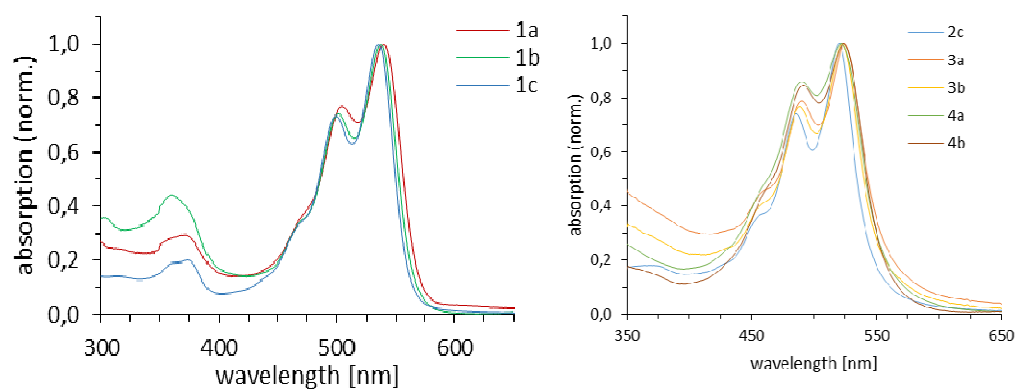
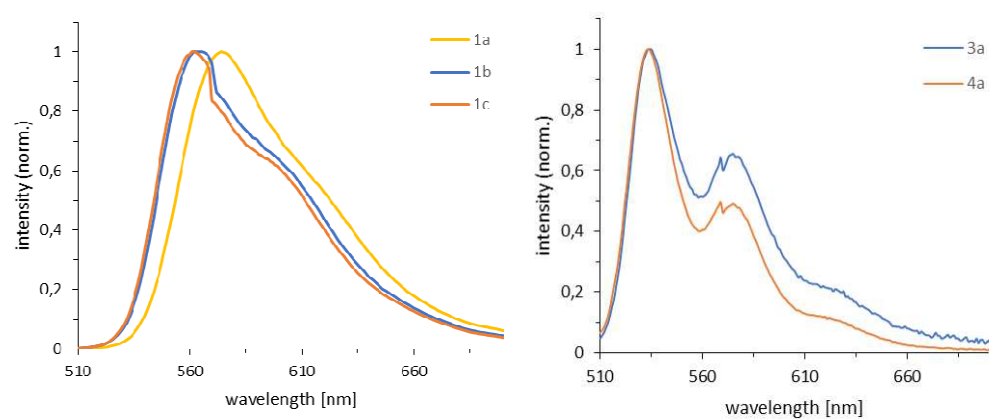


Figure S 37. IR spectra of **3a** (left) and **3b** (right) using KBr pellets.



**Figure S 38.** Normalized absorption spectra of **1a-1b** (left) and the complexes **2c, 3a-3b, 4a-4b** (right).



**Figure S 39.** Normalized emission spectra of **1a-1b** (left) and complexes **3a** and **4a** (right).

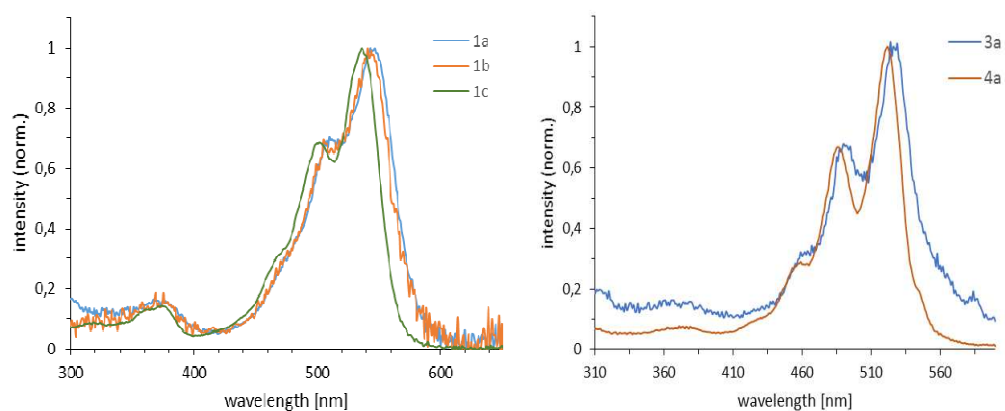


**Figure S 40.** Normalized excitation fluorescence spectra of **1a-1c** (left) and complexes **3a** and **4a** (right).